# Electronic structure of amorphous $Si_3N_4$ in the cluster-Bethe-lattice approximation

Eraldo C. Ferreira
*Departamento de Fisica, Universidade Federal Rio Grande do Norte, Natal, 59000 Rio Grande do Norte, Brasil and Instituto de Fisica, Universidade Estadual de Campinas, Campinas, 13100 São Paulo, Brazil*

C. E. T. Gonçalves da Silva
*Instituto de Fisica, Universidade Estadual de Campinas, Campinas, 13100 São Paulo, Brasil and Groupe de Physique des Solides de l'Ecole Normale Supérieure, 24 rue Lhomond, 75231 Paris Cedex 05, France*

(Received 14 June 1985)

We present a calculation of the electronic structure of amorphous $Si_3N_4$, using a model tight-binding Hamiltonian with a basis set of Si $3s$ and $3p$, and N $2s$ and $2p$ orbitals. Clusters of 13 atoms, centered at either a Si or a N atom, are constructed using structural data from crystalline $\beta$-$Si_3N_4$. These clusters are employed to generate a self-consistent transfer-matrix approximation for an infinite effective medium (Bethe lattice). The local and average densities of states are evaluated using standard one-particle Green's operator techniques. We also simulate photoemission spectra by weighting orbitally decomposed partial densities of states with appropriate photoemission cross sections. Our results are in good agreement with recent experimental data.

## I. INTRODUCTION

The compound $Si_3N_4$ crystallizes in two forms, both of hexagonal symmetry: $\alpha$-$Si_3N_4$, with four formula units per primitive cell, and $\beta$-$Si_3N_4$, with two formula units per primitive cell.[1] Recently, several techniques have been developed to produce amorphous, in general non-stoichiometric (i.e., $Si_{1-x}N_x$), alloys of Si and N, such as glow discharge of silane and ammonia[2] or chemical vapor deposition.[3] Effective intentional doping has been achieved with phosphorus and boron, to control transport properties yielding, respectively, $n$- and $p$-type samples.[4] The origin of the interest for such materials lies in their actual and potential applications in the electronics industry, as nonvolatile memory devices, and solar cells.

The structural properties of amorphous stoichiometric $Si_3N_4$ have been investigated by Aiyama *et al.*[5] and Misawa *et al.*[6] These authors have been able to establish, through x-ray and neutron scattering analysis, that the short-range order (SRO) of $a$-$Si_3N_4$ strongly resembles that of the crystalline phases, in particular that of $\beta$-$Si_3N_4$. The vibrational properties, as established by Wada *et al.*[7] offer further evidence for the similarities between the local geometric configurations of crystalline and amorphous $Si_3N_4$. The electronic properties of the crystalline phases were investigated by Ren and Ching,[8] using a first-principles orthogonalized combination of atomic orbitals approach. Robertson[9] studied the electronic properties of silicon nitrides within a simple tight-binding framework and obtained results for the densities of states for a variety of compositions, using a crystallinelike approximation. More recently, Kärcher *et al.*[10] made a systematic experimental investigation of the photoemission properties of hydrogenated and unhydrogenated amorphous $SiN_x$ with $x$ ranging up to 1.6.

The aim of the present work is to evaluate the partial and average densities of states for stoichiometric amorphous $Si_3N_4$, including the photoemission cross section for the various orbitals, in order to compare our results with those of Kärcher *et al.*[10]

In Sec. II we review briefly the relevant experimental and previous theoretical results. In Sec. III we define our model Hamiltonian and discuss our method of solution, based upon the cluster-Bethe-lattice method. In Sec. IV we present our results, and in Sec. V our conclusions.

## II. STOICHIOMETRIC SILICON NITRIDE

Structurally, the SRO in amorphous $Si_3N_4$ strongly resembles that of the local geometry of either $\alpha$-$Si_3N_4$ or $\beta$-$Si_3N_4$.[1,5,6] The average first-neighbor N-Si distances in $\beta$-$Si_3N_4$ and $a$-$Si_3N_4$ are the same, equal to 1.729 Å. The coordination numbers of N and Si are, respectively, 3 and 4 in the crystalline and 2.78 and 3.70 in the amorphous phases. There is a larger fluctuation in the nearest-neighbor (NN) distances in the amorphous (0.07 Å) than in the crystalline phase (0.02 Å). As far as next-nearest neighbors are concerned, we have to consider N(Si)N and Si(N)Si pairs. For the former, the average distances are practically the same ($\beta$: 2.835 Å; $a$: 2.83 Å), whereas for the latter they are slightly different ($\beta$: 2.98 Å; $a$: 3.01 Å). As far as the coordination numbers are concerned, we have $n_{NN}(\beta)=9$, $n_{NN}(a)=7.7$, $n_{SiSi}(\beta)=8$, $n_{SiSi}(a)=6.5$. The bond angles between any two adjoining N—Si—N bonds are, on the average, 109°, and between two adjoining Si-N-Si bonds are, on the average, 120°. For these reasons, we have chosen as basic clusters in our calculation the two 13-atom clusters shown in Fig. 1, one centered on a N atom and the other on a Si atom.

The clusters in Fig. 1 do not have, despite their sizes, any closed rings of bonds. The smallest closed ring in crystalline $Si_3N_4$ has eight bonds and extends out to the fourth-nearest neighbor. In a model Hamiltonian with NN hopping only, we thus have an "open" structure,

 

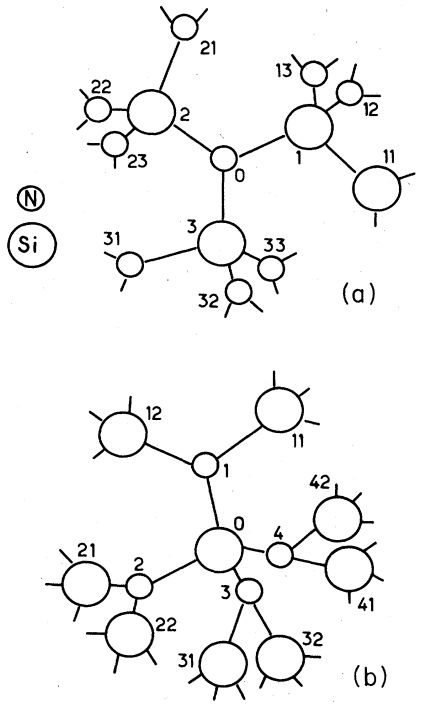


FIG. 1. Schematic representation of 13-atom clusters used to evaluate density of states: (a) N centered and (b) Si centered.

since in the Bethe lattice there are no closed rings of bonds. However, these clusters are sufficiently large to contain important structural information about the local environment, the atomic positions being deduced from the crystalline $\beta$-$Si_3N_4$ modification. The validity of this choice for the treatment of an amorphous alloy is connected to the use of the Bethe-lattice approximation[11] and is further discussed below. The photoemission results are shown in Fig. 4, where they are discussed in comparison with the theoretical curves.

The results of Ren and Ching[8] for the electronic structure of $\beta$-$Si_3N_4$ predict an indirect-gap semiconductor, with the top of the valence band off the center of the Brillouin zone. The value of the gap is dependent upon the particular model potential and basis set employed, varying between 4.72 and 7.77 eV. There are two valence bands, separated by a gap which varies between 3.36 and 5.43 eV. The upper band has a width from 8.65 (corresponding to the larger valence—conduction-band gap). The lower band has a width between 3.21 and 4.18 eV. The top of the valence band is mostly N $p$-like, whereas the bottom of the conduction band is mostly derived from Si $s$ states. The hole effective mass is fairly large ($\sim 3m_0$) due to the flatness of the top of the valence band.

Robertson has made a molecular-orbital study of the silicon nitrides, obtaining a parametrized tight-binding description of these compounds.[9] In our calculation we have used his parameters for $Si_3N_4$, as given in Table I, neglecting a second-neighbor NN $p\sigma$ interaction. The effect of this latter interaction is to introduce dispersion in an otherwise flat N $p$-like "lone-pair" orbital band. For a planar N site, corresponding to Si-N-Si angles of 120°, as

TABLE I. Tight-binding parameters employed in our calculation (from Ref. 9).

| Tight-binding parameters (eV) | | |
|---|---|---|
| Si | $E_s=-8.4$ | $E_p=-2.0$ |
| N | $E_s=-25.1$ | $E_p=-11.5$ |
| $V_{ss\sigma}=-2.28$ | | |
| $V_{ps\sigma}=-4.76$ | | |
| $V_{ps}=-2.73$ | | |
| $V_{pp\sigma}=-4.76$ | | |
| $V_{pp\pi}=-1.30$ | | |

adopted in our clusters, he finds an energy gap of 4.3 eV. He also obtains, as Ren and Ching, two valence bands; an upper one of width of the order of 13 eV, separated by a 3-eV gap from a narrow lower valence band (width: 2 eV). He finds basically the same symmetry and atomic characteristics for valence and conduction bands as Ren and Ching.[8] The hole effective mass would be infinite in the absence of the second-neighbor interaction mentioned above.

## III. MODEL HAMILTONIAN AND EVALUATION OF THE DENSITY OF STATES

We take as our basis set atomiclike Si $3s$ and $3p$, and N $2s$ and $2p$ orbitals. To each site in the structure there correspond, thus, four orbitals: one $s$-like and three $p$-like. Only nearest-neighbor hopping matrix elements, as given in Table I, are considered in the tight-binding model Hamiltonian. To evaluate the density of states we use

$$zG(z)=1+HG(z)\ , \tag{3.1}$$

where $z=E+i0^+$ is the (complex) energy, $G(z)$ is the Green's operator, and $H$ is the Hamiltonian. As is well known, the local, orbital decomposed, density of states of the $\nu$th orbital at the $i$th site is given by

$$\rho_{i\nu}(E)=-\frac{1}{\pi}\mathrm{Im}\langle i\nu\,|\,G(z)\,|\,i\nu\rangle\ . \tag{3.2}$$

The local density of states at a Si(N) site is defined by

$$\rho_{\mathrm{Si(N)}}(E)=-\frac{1}{\pi}\,\mathrm{Im}\sum_{\nu}\langle\nu\,|\,G(z)\,|\,\nu\rangle_{\mathrm{Si(N)}}\ , \tag{3.3}$$

where the angular brackets indicate a configuration average over all Si(N) sites and the sum is over the $s$ and $p$ orbitals. The total density of states is

$$\rho(E)=\tfrac{3}{7}\rho_{\mathrm{Si}}(E)+\tfrac{4}{7}\rho_N(E)\ . \tag{3.4}$$

We evaluate also an energy distribution of photoemitted electrons using the approximation

$$D(E)=\tfrac{3}{7}D_{\mathrm{Si}}(E)+\tfrac{4}{7}D_N(E)\ , \tag{3.5}$$

where

$$D_{\mathrm{Si}}(E)=-\frac{1}{\pi}\,\mathrm{Im}\sum_{\nu}\sigma_\nu\langle\nu\,|\,G(z)\,|\,\nu\rangle_{\mathrm{Si}}\ , \tag{3.6}$$

and similarly for $D_N(E)$. In (3.6), $\sigma_\nu$ is the photoemission

cross section for the $\nu$th orbital assumed energy independent.

To evaluate (3.3)—(3.6) we need to compute configuration averaged values for the diagonal matrix elements of the Green's operator. We do this in the standard way,[12] by attaching to the dangling bonds at the surface of the clusters in Fig. 1 effective fields (Bethe lattices) determined in a self-consistent way. The procedure, although cumbersome because of the number of atoms and geometry of the cluster, is straightforward. Since the positions of all equivalent atoms in the clusters are related by rotations, it is possible to show that there are only two inequivalent effective fields, one coupling N to Si and the other Si to N atoms. The calculation details are presented in the Appendix.

As shown in the Appendix, the solution described above is valid for the "crystalline" cluster, assuming identical Si—N bond lengths throughout. Otherwise, we cannot exploit symmetries which render the numerical solution of the problem manageable. The question then arises of the relevance of such a cluster to describe an amorphous material. Bond lengths and angles fluctuations in $a$-$Si_3N_4$ seem to be small, with regard to the structural data presented in Sec. II. Their main effect must be to wash out detailed structure in the density of states. This is achieved in our calculation by introducing a finite imaginary part of the energy, of the order of the experimental resolution. Hence, fine details in the density of states are lost, which is, in practice, the same effect as that of taking into account short-range structural fluctuations in the evaluation of the electronic states. Obviously, this is adequate only for such "macroscopic" quantities as the density of states, which are coarse-grain averages. Concerning the cluster-Bethe lattice approximation itself, its limitations are well known, as well as its advantages.[12] We have not attempted to evaluate charge transfers, since our Hamiltonian is not self-consistent. Self-consistency can be introduced within a tight-binding scheme, but before an evaluation of microscopic properties is undertaken we will need a better structural model as well as to take into account defects and impurities present in the amorphous state.

## IV. RESULTS

We start by presenting, in Table II, a comparison between some of our results, experimental data, and previous theoretical results. We concentrate only upon gross features of the valence bands and the semiconducting gap. The latter is predicted by the Bethe-lattice approximation to be 40% larger than the measured one. The valence-band gap is also overestimated by about 70%. On the other hand, valence bandwidths are underestimated. These are all well-known features of the approximation, which can be corrected by renormalizing the tight-binding parameters. Our results are, however, in reasonable agreement with previous theoretical calculations. The degree of precision with which the electronic structure of such a complicated material as $Si_3N_4$ can be evaluated should not lead us to expect agreement with experiment to better than 1 or 2 eV. For this reason we have not renormalized the tight-binding parameters entering into our model Hamiltonian.

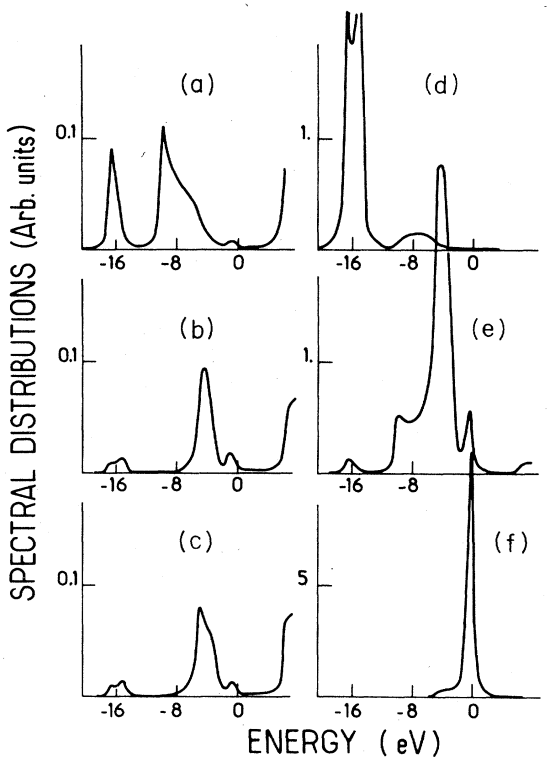


FIG. 2. Orbitally decomposed partial density of states. Si states: (a) $3s$, (b) $3p_x$ and $3p_y$, (c) $3p_z$. N states: (d) $2s$, (e) $2p_x$ and $2p_y$, (f) $2p_z$. The densities have been multiplied by the respective photoemission cross section for photon energy of 87 eV and broadened by 0.3 eV (see text for details). The curves are all plotted in the same (relative) scale. Note different scales between left and right panels.

In Fig. 2 we present the orbitally decomposed partial

TABLE II. Comparison between the main features of the valence band of $Si_3N_4$ obtained from different calculations and experiment. (All energies in eV.)

| | Experiment | Ref. 8 | Ref. 9 | This work |
|---|---|---|---|---|
| Semiconducting gap | 4.55[a] | 4.7—6.7 | 4.3 | 6.6 |
| Upper valence bandwidth | 12[b] | 8.7—10.6 | 13 | 10.6 |
| Lower valence bandwidth | 4.5[a] | 3.2—4.2 | 3 | 2.2 |
| Valence-band gap | 3[b] | 3.4—5.4 | 2 | 5.3 |

[a]Reference 13.
[b]Reference 10.

densities of states for $Si_3N_4$. Each curve has been multiplied by its relative photoemission cross section for $h\nu=87.1$ eV, normalized to $\sigma(\text{Si}, 3s)=1$; that is $\sigma(\text{Si}, 3p)=1.13$, $\sigma(\text{N}, 2s)=3.44$, and $\sigma(\text{N}, 2p)=6.88$.[10] The energy broadening is given by the imaginary part of the complex energy set at 0.3 eV. The zero of the energy is at the top of the valence band, and the curves are shown only up to the conduction-band edge, which falls at 6.6 eV. Figure 2(a) shows the Si $3s$ orbital partial density of states. The two-valence-band feature of $Si_3N_4$ is clearly visible, with a gap of about 5.3 eV between them. As already mentioned, the Bethe-lattice approximation overestimates gaps (underestimates bandwidths) unless the parameters entering the tight-binding Hamiltonian are renormalized. Figure 2(b) shows the results for the Si $3p_x$ and $p_y$ orbitals, and Fig. 2(c) shows the results for the Si $3p_z$ orbital. The contribution of the Si orbitals to the valence bands is rather small (notice the change in scale between the left and right panels of Fig. 2). The $3s$ orbital, as expected, contributes more strongly to the low-energy features. The Si states, however, contribute strongly to the bottom of the conduction band. Figure 2(d) shows the contribution of the N $2s$ orbital. This is almost completely confined to the lower valence band. Figure 2(e) shows the results for the N $2p_x$ and $p_y$ orbitals, which dominate the upper valence band. Finally, Fig. 2(f) shows the N $2p_z$ lone orbital band, concentrated at the top of the valence band.

Figure 3 shows the partial densities of states, uncorrected for photoemission cross sections, broadened by an imaginary part of the energy of 0.8 eV. All the main features of Fig. 2 are still visible, in particular the large density of states of the lone orbital band at the top of the valence band. We can also see that the contribution of the Si states is small in the lower valence band, being slightly more important near the bottom and the middle peak of the upper valence band. Again, the very strong Si character of the bottom of the conduction band is clearly visible.

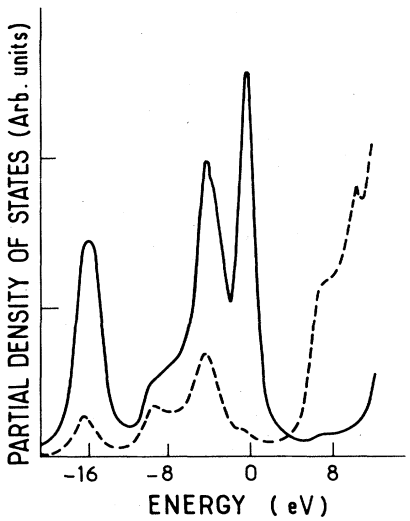


FIG. 3. Partial density of states broadened by 0.8 eV. Dashed line: Si states. Solid line: N states. The top of the valence band is at zero eV.

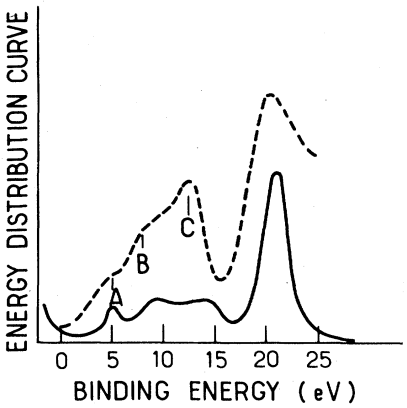


FIG. 4. Theoretical (solid line) and experimental (dashed line) energy distribution curves for photon energy 1487 eV. The experimental results were obtained by Kärchner *et al.* (Ref. 10).

Finally, in Fig. 4 we compare the total-energy-distribution curve obtained using (3.5) at a photon energy of 1487 eV, with the experimental results of Kärcher *et al.*[10] Our calculation was performed for stoichiometric $a$-$Si_3N_4$, whereas their results were obtained for $SiN_{1.5}$. This should not be very important, except perhaps for a slight enhancement of the N-derived features of the experimental spectrum in relation to the theoretical curve. The broadening of the latter was obtained using an imaginary part of the energy of 0.8 eV, in accordance with the experimental resolution of 0.86 eV. We aligned the experimental peak $A$ and the theoretical peak due to the N $2p$ lone-pair band. Peak $B$ corresponds thus to N $2p_x$ and $p_y$, and Si $3p$—derived states, whereas peak C is mostly N $2p_x$ and $p_y$ with some admixture of Si $3s$. There is no evidence for a fourth peak in the upper valence band, as deduced by Kärcher *et al.* from Robertson's calculation.[9,10] Therefore, the cluster Bethe-lattice approximation yields results in better agreement with experiment than previous calculations. The lowest peak is, as discussed before, N $2s$. There are two obvious discrepancies between theory and experiment, as shown in Fig. 4. First, the relative positions of the peaks are different, the theoretical ones being further apart than the experimental ones. This could be corrected, for instance, by a different choice of parameters than that of Table I. However, given the nature of our model and the approximations we employ, we did not attempt this fit. What we have shown is that a relatively simple calculation can account for some of the main spectral features of the experimental curves. Second, the relative intensities of peaks $A$, $B$, and $C$ are quite different. This is due, in part, to the underestimation of the lone-pair orbital bandwidth in our calculation, which leads to an enhancement of the height of the peak $A$. It is also due to the Bethe-lattice approximation, which is not designed to reproduce precise features of the density of states. In addition, there are matrix-element effects which have not been fully taken into account.

## V. CONCLUSION

We have presented a calculation of the local density of states and energy-distribution curve for stoichiometric

amorphous $Si_3N_4$ based upon a model tight-binding Hamiltonian. The basis set includes Si and N $s$- and $p$-like valence orbitals, and nearest-neighbor hopping is considered. Clusters of 13 atoms, N and Si centered, are employed in conjunction with the Bethe-lattice approximation to determine the electronic structure. Our results for the valence-band density of states are in good agreement with recently published data. We have thus shown the usefulness of the Bethe-lattice approximation to deal with fairly complicated materials, which even in their crystalline form pose nontrivial calculational problems due to their low symmetry and high number of atoms per primitive cell. The same method can be employed to study the amorphous $SiN_x$ alloys as a function of the composition $x$, although the lack of structural information concerning the Si and N local environment as $x$ increases poses some difficulties. We are investigating this problem.

## ACKNOWLEDGMENTS

One of us (C.E.T.G.dS.) would like to thank the Conselho Nacional de Desenvolvimento Cientifico e Tecnologico (CNPq) for financial support and acknowledge the hospitality of Dr. Michel Voos and the members of his group at the Ecole Normale Supérieure, where this work was concluded. The authors would also like to thank the members of the photovoltaic-cell research group at Universidade Estadual de Campinas, in particular Professor I. Chambouleyron, for bringing this problem to their attention, as well as for several discussions. This work was supported in part by Fundação de Amparo a Pesquisa do Estado de São Paulo (FASESP). E.C.F. was also supported by Coordenação de Aperfeicoamento de Pessoal do Ensino Superior (CAPES).

## APPENDIX

Let us write (3.1) in matrix form:

$$zG_{ij}=\delta_{ij}+\sum_k H_{ik}G_{kj} , \tag{A1}$$

where $G_{ij}$ and $H_{ik}$ are $4\times4$ matrix representations, respectively, of the operators $G$ and $H$ in the $\{|i\nu\rangle\}$ basis, where $i$ is the site index and $\nu$ is the orbital index. Taking a N-centered cluster, in the notation of Fig. 1, we obtain

$$(z-H_{\mathrm{N}})G_{00}=1+\sum_{k=1}^{3} H_{0,k}G_{k0} , \tag{A2}$$

$$(z-H_{\mathrm{Si}})G_{i0}=H_{i0}G_{00}+\sum_{k=1}^{2} H_{ij,ik}G_{ik,0} , \tag{A3}$$

$$(z-H_{\mathrm{N}})G_{ij,0}=H_{ij,i}G_{i0}+\sum_{k=1}^{3} H_{ij,ijk}G_{ik,0} . \tag{A4}$$

In (A2)—(A4), $H_{\mathrm{N}}$ and $H_{\mathrm{Si}}$ are the intrasite Hamiltonian matrices and, otherwise noted, $i,j,k=1,2,3$.

We define the transfer matrices:

$$T_{(ij)k}=G_{ijk,0}G_{ij,0}^{-1} , \tag{A4}$$

$$T_i=G_{i0}G_{00}^{-1} . \tag{A5}$$

Since

$$H_{ij,ijk}=S_{(ij)k}H_{0,k}S_{(ij),k}^{-1} , \tag{A6}$$

where $S$ is unitary, we can show that

$$T_{(ij)k}=S_{(ij)k}T_iS_{(ij)k}^{-1} . \tag{A7}$$

We also have

$$H_{0,l}=S_lH_{0,1}S_l^{-1},\quad l=2,3 \tag{A8}$$

so that

$$T_l=S_lT_1S_l^{-1},\quad l=2,3 . \tag{A9}$$

Finally, by requiring the identity of the solution of (A2) with $G_{k,0}=T_kG_{0,0}$ and of (A2)—(A4) with $G_{ijk,0}=T_{(ij)k}G_{ij,0}$ we obtain a self-consisting condition for $T_1$:

$$T_1=\left[z-H_{\mathrm{Si}}-\sum_{j=1}^{3} H_{1,1j}\left[z-H_{\mathrm{N}}-\sum_{k=1}^{2} H_{1j,1jk}S_{(ij)k}T_1S_{(ij)h}^{-1}\right]^{-1}H_{1j,1}\right]^{-1}H_{10} , \tag{A10}$$

which is solved iteratively.

The simplest way to understand (A6) is to remember that under a rotation, in the Slater-Koster formalism, $H_{ss}$ transforms like a scalar, $H_{sp}$ and $H_{ps}$ like vectors, and $H_{pp}$ like a second-rank tensor. The matrices $S$ are then simply:

$$S=\begin{bmatrix}1 & 0\\ 0 & R\end{bmatrix} , \tag{A11}$$

where $R$ is the $3\times3$ rotation matrix which takes the unit vector in the direction $0k$ into the unit vector in the direction $(ij,ijk)$. Crucial to this symmetry argument is the invariance of the bond lengths.

Finally, we obtain

$$G_{00}=\left[z-H_{\mathrm{N}}-\sum_{k=1} H_{0,k}T_k\right]^{-1} , \tag{A12}$$

and similarly for a Si-centered cluster.

[1]R. Wyckoff, *Crystal Structures* (Interscience, New York, 1964), Vol. 2.
[2]L. Ley, R. Kärcher, and R. L. Johnson, Phys. Rev. Lett. **53**, 710 (1984).
[3]C.-E. Morosanu, Thin Solid Films **65**, 171 (1980).
[4]F. Alvarez and I. Chambouleyron, Sol. Energy Mater. **10**, 151 (1984).
[5]T. Aiyama, T. Fukunaga, K. Niihara, T. Hirai, and K. Suzuki, J. Non-Cryst. Solids **33**, 131 (1979).
[6]M. Misawa, T. Fukunaga, K. Niihara, T. Hirai, and K. Suzuki, J. Non-Cryst. Solids **34**, 313 (1979).
[7]N. Wada, S. A. Solin, J. Wong, and S. Prochazka, J. Non-Cryst. Solids **43**, 7 (1981).
[8]S.-Y. Ren and W. Y. Ching, Phys. Rev. B **23**, 5454 (1981).
[9]J. Robertson, Philos. Mag. B **44**, 215 (1981).
[10]R. Kärcher, L. Ley, and R. L. Johnson, Phys. Rev. B **30**, 1896 (1984).
[11]R. B. Laughlin and J. D. Joannopoulos, Phys. Rev. B **20**, 5228 (1979).
[12]J. D. Joannopoulos and M. L. Cohen, Solid State Phys. **31**, 71 (1976).
[13]J. Bauer, Phys. Status Solidi A **39**, 411 (1977).